

Reaction spectroscopy at fragmentation beam energies – recent advances in studies of two-nucleon removal

J.A. Tostevin^{1,2,a}

¹ Department of Physics, School of Electronics and Physical Sciences, University of Surrey, Guildford, Surrey GU2 7XH, UK
² Department of Nuclear Physics, Research School of Physical Sciences and Engineering, The Australian National University, Canberra, ACT 0200, Australia

Received: January 31, 2007

Abstract. Final-state-exclusive two-nucleon removal reaction data from fast fragmentation beams can provide a demanding test of the microscopic two-nucleon transition densities calculated from large-basis shell model wave functions. The sensitivity of measured partial cross sections to pairing and other correlations is discussed. It is also suggested that the widths of the momentum distributions of these partial cross sections will exhibit a strong dependence on the final-state of the residue and the projectile structure.

PACS. 25.60.-t Reactions induced by unstable nuclei – 23.40.Hc Relation with nuclear matrix elements and nuclear structure

1 Introduction

Exotic nuclei are revealing a complex evolution of nucleon single-particle states with increasing neutron-proton asymmetry. Final-state-exclusive single nucleon knockout reactions at fragmentation energies, measured using a combination of particle and γ -ray spectroscopy, continue to play a key part in understanding this evolution, e.g. [1,2]. Their large intrinsic cross sections and high experimental efficiency and selectivity, allow the mapping of the energies, angular momenta, order and strengths of single-particle configurations at both the tightly-bound and the weakly-bound nucleon Fermi surfaces, e.g. [3,4]. Furthermore, they have been shown to provide quantitative spectroscopic information [5], a long-standing ambition of direct reaction methods. Though more complicated, fast two-nucleon knockout reactions may provide unique additional information, particularly on the role of nucleon correlations and pairing in asymmetric systems.

That two-proton removal from neutron rich nuclei (represented in figure 1) takes place as a sudden direct reaction was observed at the NSCL [6]. First analyses were presented at RNB6 [7] for the reaction $^{28}\text{Mg} \rightarrow ^{26}\text{Ne} (J^\pi)$ at 83.2 MeV on a ^9Be target. Very recent measurements of two-neutron knockout, from intermediate-energy beams of ^{34}Ar , ^{30}S , and ^{26}Si , confirm this observation on the neutron-deficient side of the nuclear chart [8]. As has also been pointed out recently [9,10], access to both one- and two-nucleon removal data gives greater insight into

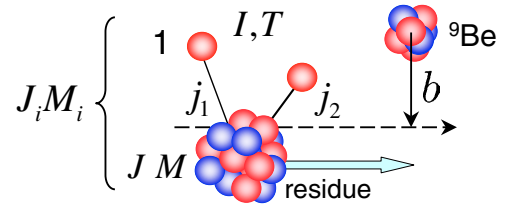


Fig. 1. Representation of the direct two-nucleon knockout mechanism on a light target at an impact parameter b .

structures at shell or subshell gaps, including transitions involving removal of the nucleons from above and across a shell gap – the latter being revealed by the population of final states of opposite parity [10].

Here we discuss two aspects of two-nucleon removal – the role of correlations and a first estimation of the reaction residue partial momentum distributions.

2 Reaction theory methodology

The few-body reaction theory of two nucleon knockout [11,12] interfaces the eikonal reaction dynamics with the microscopic two nucleon transition densities from large basis shell model wave functions. In a transition from a spin $J_i = 0$ projectile to a given residue (or core, c) final state JM , the two-nucleon transition density is

$$F_J^M(1, 2) = \sum_{j_1 j_2} (-1)^{J+M} C(j_1 j_2 J) / \hat{J} [\phi_{j_1} \otimes \phi_{j_2}]_{J-M} \quad (1)$$

where the $C(j_1 j_2 J)$ are the shell model two-nucleon amplitudes (TNA) of the contributing antisymmetrized

^a Supported by the United Kingdom Engineering and Physical Sciences Research Council (EPSRC) under Grant No. EP/D003628.

e-mail: j.tostevin@surrey.ac.uk

two-nucleon configurations $[\phi_{j_1} \otimes \phi_{j_2}]$. The partial cross sections for two-nucleon removal are the integrals over projectile impact parameters

$$\sigma_J = \frac{1}{2J+1} \sum_M \int db |S_c|^2 \langle F_J^M | \hat{O}(1,2) | F_J^M \rangle \quad (2)$$

where $\hat{O}(1,2)$ is the relevant two-nucleon removal operator. In the calculations discussed here [9,11,12] the dominant cross section contributions arise from the absorptive terms

$$\begin{aligned} \hat{O}(1,2) = & (1 - |S_1|^2)(1 - |S_2|^2) \\ & + |S_1|^2(1 - |S_2|^2) + (1 - |S_1|^2)|S_2|^2 \end{aligned} \quad (3)$$

where the S_α are the eikonal model S-matrices for each particle ($\alpha = c, 1, 2$) with the target. The first term describes the absorption (stripping) of both nucleons by the target and the second and third terms describe events where one nucleon is absorbed, the $(1 - |S_j|^2)$ factor, and the other scatters elastically, the $|S_i|^2$ factor, from the target. These elastic (diffraction) factors must however be corrected. For both nucleons, $i = 1, 2$, we must replace

$$|S_i|^2 \rightarrow S_i^* \left[1 - \sum_{j'm'} |\phi_{j'}^{m'}|(\phi_{j'}^{m'}) \right] S_i, \quad (4)$$

to remove (one-nucleon knockout) cross section due to elastic interactions that leave the diffracted nucleon and the residue in bound states $\phi_{j'}$. Details are presented elsewhere [11,12].

3 Two-nucleon spatial correlations

The two-nucleon removal cross section, equation 2, is not directly nucleon spin state selective [11,13]. As the projectile and the target collide at high-speed the target will bore a cylindrical hole through the surface of the projectile, in the direction of the incident beam, at an impact parameter b , figure 2(a). Both one- and two-nucleon removal events involve only such grazing collisions – those with smaller b resulting in much greater mass removal and strong absorption of the mass $A-1$ and $A-2$ residues.

Though not pair-spin selective, it is clear that two-nucleon removal yields will probe the spatial probability (proximity) of pairs of like-nucleons that contribute to a given J^π transition. We can thus gain insight into the reaction (and observational) sensitivity to details of the microscopic two-nucleon wave functions, accessible through these spatial correlations, by interrogating the sampled volume of figure 2(a).

We consider the J -dependence of (i) the position probabilities, $P_J(\mathbf{s}_1, \mathbf{s}_2)$, that two (point) nucleons (1, 2) will be found with values of s_1 and s_2 (near the projectile surface) with an angular separation φ , see figure 2(b), and (ii) the associated differential probabilities $P_J(\mathbf{s}_1, \mathbf{s}_2, K)$ that their total z -component of momentum, and hence

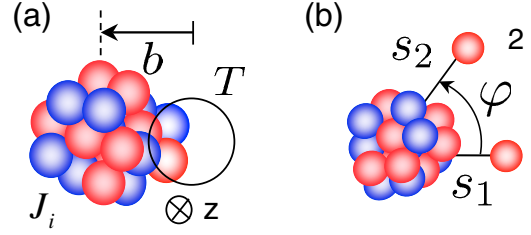


Fig. 2. (a) Representation of the cylindrical volume probed by the target (T) in the direct two-nucleon knockout mechanism. (b) The two-removed-nucleon position coordinates defined in the (impact parameter) plane normal to the beam direction.

that of the residue, is K . These momenta are referred to the rest frame of the projectile. The relevant nucleon positions s_1 and s_2 are in the plane perpendicular to the beam direction and the position probabilities $P_J(\mathbf{s}_1, \mathbf{s}_2)$ are integrated along the incident beam direction, which is defined to be the z -axis, i.e.

$$P_J(\mathbf{s}_1, \mathbf{s}_2) \propto \sum_M \int dz_1 \int dz_2 \langle F_J^M(1,2) | F_J^M(1,2) \rangle_{sp}. \quad (5)$$

Here $\langle \dots \rangle_{sp}$ denotes the integration over spin variables. If the nucleons were completely uncorrelated then of course

$$P(s_1, s_2) \propto \sum_{mm'} \int dz_1 \langle \phi_j^m | \phi_j^m \rangle_{sp} \int dz_2 \langle \phi_j^{m'} | \phi_j^{m'} \rangle_{sp} \quad (6)$$

which is then both J and φ independent.

4 Results for partial cross sections

Several correlations affect the (surface) position probability density of the two nucleons and their removal cross section. Going from the φ - and J -independent fully uncorrelated limit to including a single two-nucleon configuration $C(jjJ)$, via equation (1), one must include those (essential but trivial) correlations from angular momentum coupling/antisymmetrisation of the nucleons. The effects on the $P_J(s_1, s_2, \varphi)$ are important, shown in figure 3(a) for a $[d_{5/2}]^2$ proton pair in ^{28}Mg . The dependence on φ will clearly enhance 0^+ , suppress 4^+ , and have little effect on 2^+ final state populations, compared to the uncorrelated limit. This will be a very general feature. These qualitative expectations, based on interrogating a few points in the sampled volume of figure 2(a), are confirmed by the full knockout cross section calculations, of section 2, shown in part (b) of the figure. Here the inclusive cross sections have been normalised to the experimental value, $\sigma_{\text{incl}} = 1.50(10)$ mb [6] and the measured 2_1^+ and 2_2^+ cross sections have been summed, shown as 2^+ . These calculations use the $C(jjJ)$ appropriate for a pure $[d_{5/2}]^2$ pair, $\sqrt{4/3}$, $\sqrt{5/3}$ and $\sqrt{3}$ for 0^+ , 2^+ and 4^+ transitions, respectively [11]. It follows that uncorrelated cross sections are in the ratio 4:5:9.

Beyond these effects are the correlations specific to the many-body shell model which will (i) redistribute the

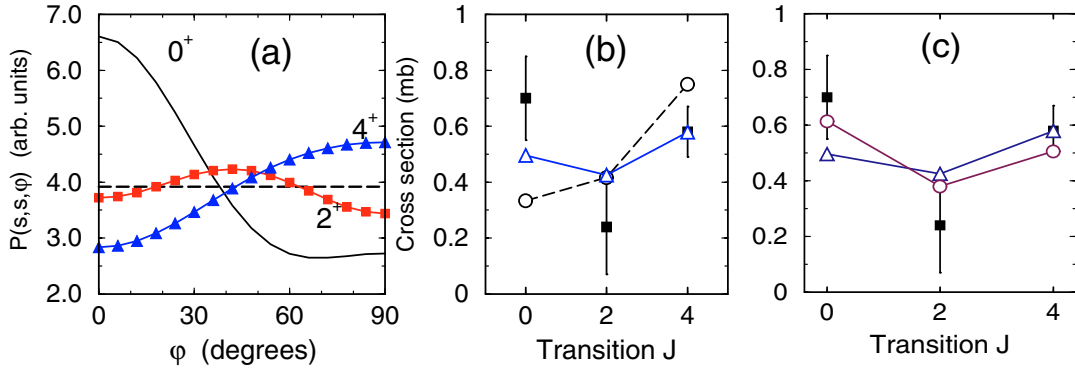


Fig. 3. (a) ϕ -dependence of the two nucleon position probabilities $P_J(s, \phi)$, with $s = 2.5$ fm, for $J = 0^+$, 2^+ and 4^+ transitions, assuming $[d_{5/2}]^2$ two-proton removal from ^{28}Mg . The curves show the changes relative to the uncorrelated limit (the constant dashed line). (b) The corresponding 0^+ , 2^+ and 4^+ partial cross sections (open triangles) are compared with values for an uncorrelated pair (open circles) and with the experimental data of [6] (filled squares) at 82.3 MeV/nucleon. (c) Partial cross sections from the full shell model wave functions (open circles) compared to those for a $[\pi d_{5/2}]^2$ configuration (open triangles, as in (b)).

strengths (and phases) of the TNA, $C(j_1 j_2 J)$, between a number of active two-nucleon configurations, and between the final states J^π , and (ii) introduce the coherence of these configurations implicit in the full calculation of equation (5). Figure 3(c) shows the results for the partial cross sections when including these additional effects. Even for the ^{28}Mg system shown, which is dominantly $[d_{5/2}]^2$, there is a significant further enhancement of the 0^+ ground-state to ground-state knockout. These coherent (pairing) effects are very much more significant in systems with a greater mixing of orbital components in their ground state: these include the case of two-proton knockout from ^{44}S , discussed in [9].

This same enhancement of the 0^+ transitions, over uncorrelated estimates, is seen very clearly for the three recent measurements of two-neutron knockout from nuclei in the proximity of the proton dripline. These were studied using intermediate-energy beams of neutron-deficient ^{34}Ar , ^{30}S , and ^{26}Si [8]. These are shown in figure 4 in terms of the measured and calculated (0^+) ground state branching ratios. The fully-correlated calculations (filled

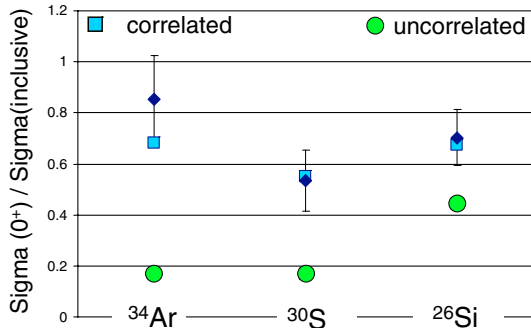


Fig. 4. Ground state branching ratios of the two-neutron removal reactions from ^{26}Si , ^{30}S and ^{34}Ar obtained (i) from experiment (filled diamonds), and calculated assuming (ii) two uncorrelated neutrons (circles), and (iii) the many-body shell model wave functions (squares). Adapted from [8].

square points), that use the two-nucleon transition densities calculated from the large-basis (USD) shell model [14], are seen to be in excellent agreement with the data.

5 Results for partial momentum distributions

To date, inclusive but not partial residue momentum distributions have been measured in the case of two-nucleon knockout reactions [6, 10]. In one nucleon removal the partial momentum distributions are a powerful spectroscopic diagnostic, having widths sensitive to the angular momentum of the removed nucleons and to the final states. In two-nucleon knockout, in the limit that the two nucleons are completely uncorrelated, the predicted momentum distributions are obtained by convoluting the distributions for the removal of each nucleon individually [6]. The inclusive distributions, when further convoluted with the incident beam momentum profiles, are consistent with the broad distributions observed in [6, 10] within the limited statistics of the experiments. A first estimate of the sensitivity of two-nucleon knockout partial momentum distributions to the transition and residue final state can be obtained by now looking at the momentum content of the correlated two-nucleon wave functions within the volume sampled by the target nucleus, figure 2(a). We thus calculate the probability $P_J(s_1, s_2, K)$ that, with the two nucleons at positions s_1 and s_2 in the plane perpendicular to the beam direction, figure 2(b), the residue will be found with a z -component of momentum $K = -(k_1 + k_2)$. Here k_1 and k_2 are the z -components of momentum of the two struck nucleons, and all momenta are referred to the rest frame of the projectile. Explicitly,

$$P_J(s_1, s_2, K) = \sum_M \left\langle \int dk_1 \int dk_2 \delta(K + k_1 + k_2) \times \left| \int dz_1 \int dz_2 e^{ik_1 z_1} e^{ik_2 z_2} F_J^M \right|^2 \right\rangle_{sp}. \quad (7)$$

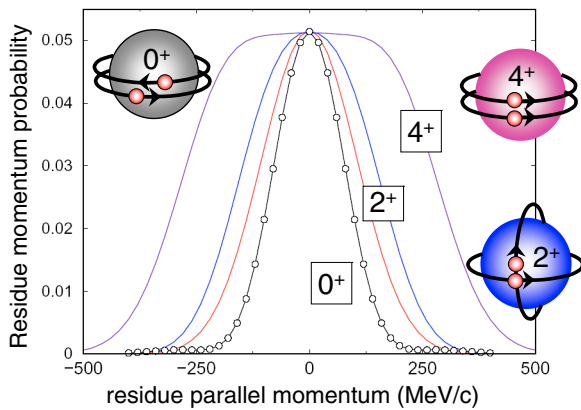


Fig. 5. Calculated residue momentum probabilities $P_J(s, s, \varphi, K)$ (normalised to unity at $K = 0$) for $s = 2.5$ fm and $\varphi = 10$ degrees. The results are for two-proton removal to the 0^+ , 2_1^+ , 4^+ and 2_2^+ ^{26}Ne final states at 82.3 MeV per nucleon. The graphics show schematically the two nucleon configurations expected to lead to the widest components of the observed distributions – those with velocities parallel or antiparallel to the beam direction, which is assumed to be from left to right.

The resulting residue distributions, for $s_1 = s_2 = 2.5$ fm and $\varphi = 10$ degrees, are shown in figure 5 for $^{28}\text{Mg} \rightarrow ^{26}\text{Ne}(J^\pi)$ at 83.2 MeV on a ^9Be target. They display a strong transition dependence, suggesting that partial momentum distributions in two-nucleon knockout reactions will also have high spectroscopic value.

The widest components of the residue distributions are expected to arise from components in the wave function with nucleon velocities parallel to, or antiparallel to the beam direction. As is shown schematically by the graphics in the figure, and because the $^{28}\text{Mg} \rightarrow ^{26}\text{Ne}(J^\pi)$ reaction used is predominantly $[d_{5/2}]^2$ proton removal, one would expect the 2^+ and 4^+ final state residue distributions to be approximately once and twice the width, respectively, of that for a single $[d_{5/2}]$ proton removal. This is approximately what is observed. Also clear is that the narrow distribution calculated for the 0^+ transition is the result

of like-nucleon pairing. Measurements are needed to test these suggestions.

6 Summary comments

Analyses of two-nucleon removal from exotic projectiles, first reported at RNB6, have advanced very significantly. It is now clear that, as for single-nucleon removal, comparisons of calculations that combine reaction theory and shell-model transition densities with partial cross sections measurements can assess the effects of nucleon pairing and of small admixtures in the shell model wave function – a consequence of coherence in the reaction mechanism. It is further suggested that partial momentum distributions of reaction residues, unmeasured so far, could provide both a clear signal of the nature of specific transitions and their J . They will also provide insight and further assessment of the reaction mechanism and of microscopic two-nucleon transition densities for some of the most exotic nuclei.

References

1. J.R. Terry et al., Phys. Lett. B (2006) (in press)
2. S.D. Pain et al., Phys. Rev. Lett. **96**, 032502 (2006)
3. P.G. Hansen, J.A. Tostevin, Annu. Rev. Nucl. Part. Sci. **53**, 219 (2003)
4. A. Gade et al., Phys. Rev. Lett. **93**, 042501 (2004)
5. B.A. Brown et al., Phys. Rev. C **65**, 061601(R) (2002)
6. D. Bazin et al., Phys. Rev. Lett. **91**, 012501 (2003)
7. D. Bazin et al., Nucl. Phys. A **746**, 173 (2004); J.A. Tostevin, Nucl. Phys. A **746**, 166 (2004)
8. K. Yoneda et al., Phys. Rev. C **74** (2006) (in press)
9. J. Fridmann et al., Nature **435**, 922 (2005); Phys. Rev. C **74** (2006) (in press)
10. A. Gade et al., Phys. Rev. C **74** (2006) (in press)
11. J.A. Tostevin, G. Podolyák, B.A. Brown, P.G. Hansen, Phys. Rev. C **70**, 064602 (2004)
12. J.A. Tostevin et al. (2006) (in preparation)
13. J.A. Tostevin, J. Phys. Conf. Ser. (in press)
14. B.A. Brown, B.H. Wildenthal, Annu. Rev. Nucl. Part. Sci. **38**, 29 (1998)